

Mesoscopic Ensembles of Polar Bosons in Triple-Well Potentials

T. Lahaye,^{1,2,3} T. Pfau,³ and L. Santos⁴

¹Université de Toulouse, UPS, Laboratoire Collisions Agrégats Réactivité, IRSAMC; F-31062 Toulouse, France

²CNRS, UMR 5589, F-31062 Toulouse, France

³Physikalisches Institut, Universität Stuttgart, Pfaffenwaldring 57, 70550 Stuttgart, Germany

⁴Institut für Theoretische Physik, Leibniz Universität Hannover, Appelstrasse 2 D-30167, Hannover, Germany
(Received 27 November 2009; revised manuscript received 25 February 2010; published 28 April 2010)

Mesoscopic dipolar Bose gases in triple-well potentials offer a minimal system for the analysis of the nonlocal character of the dipolar interaction. We show that this nonlocal character may be clearly revealed by a variety of possible ground-state phases. In addition, an appropriate control of short-range and dipolar interactions may lead to novel scenarios for the dynamics of polar bosons in lattices, including the dynamical creation of mesoscopic quantum superpositions, which may be employed in the design of Heisenberg-limited atom interferometers.

DOI: 10.1103/PhysRevLett.104.170404

PACS numbers: 03.75.Kk, 03.75.Lm

Interparticle interactions are crucial in quantum gases [1]. They can usually be described by a short-range isotropic potential proportional to the scattering length a . Recently, dipolar quantum gases, in which the long-range and anisotropic dipole-dipole interaction (DDI) between magnetic or electric dipole moments plays a significant or even dominant role, have attracted a lot of interest as they show fascinating novel properties [2,3]. To date, dipolar effects have been observed experimentally only with atomic magnetic dipoles, being particularly relevant in Bose-Einstein condensates (BECs) of ^{52}Cr where exciting new physics has been observed [4–7]. Dipolar effects have also been reported in spinor BECs [8], and in ^{39}K and ^7Li BECs with $a = 0$ [9,10]. Recent experiments with polar molecules [11,12] open fascinating perspectives towards the realization of highly dipolar gases.

Although a very clear and direct demonstration of the anisotropy of the DDI was given by the d -wave collapse of a Cr BEC [6,7], an equivalently obvious “visual” proof of the nonlocal character of the DDI is still missing. Such a nonambiguous qualitative evidence of the nonlocal character of the dipolar interaction could be provided in principle by the observation of novel quantum phases (super-solid, checkerboard) in optical lattices [13]. However, the unambiguous detection of such phases is far from trivial, as is the preparation of the ground state of the system due to a large number of metastable states [14].

In this Letter, we investigate a minimal system, namely, a mesoscopic sample of dipolar bosons in a triple-well potential, which minimizes these restrictions, while still presenting clear visual nonlocal features (see “phase” B below). Nondipolar BECs in double-well potentials have allowed for the observation of Josephson oscillations and nonlinear self-trapping [15], showing clearly that “slicing” a BEC dramatically enhances the effects of interactions. The two-well Josephson physics is affected quantitatively (although not qualitatively) by the DDI [16,17] (the DDI may induce, however, significant intersite

effects in coupled 1D and 2D bilayer systems [18–20]). On the contrary, as we show below, the DDI does introduce qualitatively novel physics in the Josephson-like dynamics in three-well systems. We discuss how the DDI leads to various possible ground states, which may visually reveal the nonlocality of the DDI. In addition, we show how this nonlocality leads to a peculiar quantum dynamics characterized by striking new phenomena, including the dynamical formation of mesoscopic quantum superpositions (MQS). MQSs produced in cavity QED or with trapped ions [21] require complex manipulations, whereas in the present system they arise naturally, similar to the MQSs obtained in BECs with attractive interactions in double wells [22,23] or lattices [24]. We then comment on the design of four-site Heisenberg-limited atom interferometers using the dynamical creation of MQS, and finally discuss possible experimental scenarios.

We consider N dipolar bosons in a three-well potential $V_{\text{trap}}(\mathbf{r})$ [Fig. 1(a)]. The wells are aligned along the y axis, separated by a distance ℓ and an energy barrier V_0 . The bosons are polarized by a sufficiently large external field, with a dipole moment \mathbf{d} along a given direction. The lattice potential is strong enough compared to other energies (in particular, the interaction energies) such that the on-site wave functions $\phi_{i=1,2,3}(\mathbf{r})$ are fixed, being independent of the number of atoms per site. For a large enough V_0 we may assume $\phi_i(\mathbf{r}) = \phi(\mathbf{r} - \mathbf{r}_i)$, where \mathbf{r}_i is the center of site i . In addition we may assume ϕ to be a Gaussian with

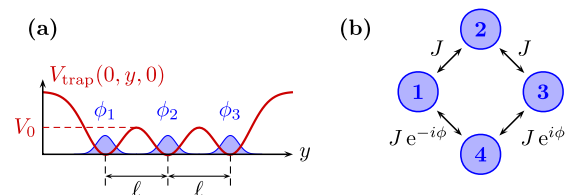


FIG. 1 (color online). (a) Schematic view of the three-well system. (b) MQS interferometer with four wells (see text).

widths $\sigma_{x,y,z}$. We limit to the case where σ_y is small enough with respect to ℓ so that the sites are well defined. Reexpressing the bosonic field operator as $\hat{\psi}(\mathbf{r}) = \sum_{i=1}^3 \phi_i(\mathbf{r})\hat{a}_i$, we may write the Hamiltonian as

$$\hat{H} = -J[\hat{a}_2^\dagger(\hat{a}_1 + \hat{a}_3) + \text{H.c.}] + \frac{U_0}{2} \sum_{i=1}^3 \hat{n}_i(\hat{n}_i - 1) + U_1 \left[\hat{n}_1\hat{n}_2 + \hat{n}_2\hat{n}_3 + \frac{1}{\alpha} \hat{n}_1\hat{n}_3 \right], \quad (1)$$

where $J = -\int d\mathbf{r} \phi_1(\mathbf{r})[-\hbar^2\nabla^2/2m + V_{\text{trap}}(\mathbf{r})]\phi_2(\mathbf{r})$ is the hopping rate, $U_0 = g \int |\phi_1|^4 d\mathbf{r} + \int |\phi_1(\mathbf{r})|^2 |\phi_1(\mathbf{r}')|^2 \times U_{\text{dd}}(\mathbf{r}-\mathbf{r}') d\mathbf{r} d\mathbf{r}'$ characterizes the on-site interactions, $U_1 = \int |\phi_1(\mathbf{r})|^2 |\phi_2(\mathbf{r}')|^2 U_{\text{dd}}(\mathbf{r}-\mathbf{r}') d\mathbf{r} d\mathbf{r}'$ is the coupling constant for nearest-neighbor DDI, and $\hat{n}_j = \hat{a}_j^\dagger \hat{a}_j$. In the previous expressions $g = 4\pi\hbar^2 a/m$ is the coupling constant for the short-range interactions, with a the s -wave scattering length. The DDI is given by $U_{\text{dd}}(\mathbf{r}) = d^2(1 - 3\cos^2\theta)/r^3$, where θ is the angle between \mathbf{r} and \mathbf{d} , $d^2 \equiv \mu_0\mu^2/(4\pi)$ for magnetic dipoles (μ is the magnetic dipole moment) or $d^2 \equiv \bar{d}^2/4\pi\epsilon_0$ for electric dipoles (\bar{d} is the electric dipole moment). The parameter α in Eq. (1) depends on the geometry of $V_{\text{trap}}(\mathbf{r})$ ($\alpha = 8$ if the wave functions are well localized in all directions compared to ℓ , and decreases towards $\alpha = 4$ when $\sigma_x/\ell \rightarrow \infty$ [25]). In the following we focus on the localized case, i.e., $\alpha = 8$, but all results remain valid for $4 \leq \alpha \leq 8$. Finally, note that U_0 results from short-range interactions and DDI, and that the ratio between U_0 and U_1 may be easily manipulated by means of Feshbach resonances, by modifying the dipole orientation \mathbf{d} and by changing ℓ [25].

Since $\sum_i \hat{n}_i = N$ is conserved by (1), we may rewrite \hat{H} [up to a global energy $U_0 N(N-1)/2$] as an effective Hamiltonian without on-site interactions:

$$\hat{H} = -J[\hat{a}_2^\dagger(\hat{a}_1 + \hat{a}_3) + \text{H.c.}] + (U_1 - U_0)\hat{n}_2[\hat{n}_1 + \hat{n}_3] + \left(\frac{U_1}{8} - U_0\right)\hat{n}_1\hat{n}_3. \quad (2)$$

The gross structure of the ground-state diagram is understood from the $J = 0$ case, where the Fock states $|n_1, n_3\rangle$ are eigenstates of \hat{H} , with energy $E(n_1, n_3)$ (since N is conserved, the Fock states are defined by $n_{1,3}$). The minimization of E provides four classical “phases.” For $U_0 > 0$ and $U_1 \leq 8U_0/15$, and $U_0 < 0$ and $U_1 < -8|U_0|$, phase (A) occurs, with $n_1 = n_3 = \lfloor \bar{n}/2 \rfloor$ with $\bar{n} \equiv 16N(U_0 - U_1)/(24U_0 - 31U_1)$ (where $\lfloor \cdot \rfloor$ denotes the integer part). Phase (B) appears for $U_0 > 0$ and $8U_0/15 \leq U_1 \leq 8U_0$, being characterized by $n_1 = n_3 = N/2$. For $U_0 > 0$ and $U_1 > 8U_0$, and $U_0 < 0$ and $U_1 > -|U_0|$, phase (C) occurs, with $n_2 = N$ (actually states with $n_i = N$ are degenerated, but the degeneracy is broken by tunneling which favors $n_2 = N$). Finally, phase (D) occurs for $U_0 < 0$ and $8U_0 < U_1 < U_0$, being characterized by a broken symmetry, with two degenerated states with $n_1 = \lfloor \bar{n} \rfloor$, $n_3 = 0$ and vice versa.

Figure 2(a) shows $\langle \hat{n} \rangle/N$, with $\hat{n} = \hat{n}_1 + \hat{n}_3$ for $N = 18$. We can see that phases (A)–(D) describe well the gross structure of the ground-state diagram [a similar graph shows, as expected, that the (D) phase shows large fluctuations $\Delta \hat{\delta}$ in $\hat{\delta} = \hat{n}_1 - \hat{n}_3$]. However, tunneling is relevant at low $|U_0|$ and $|U_1|$ and at the phase boundaries. In general, the system is in a quantum superposition of different Fock states $|\psi\rangle = \sum_{n_1=0}^N \sum_{n_3=0}^{N-n_1} C(n_1, n_3)|n_1, n_3\rangle$. Figure 2(b) depicts $\Delta \hat{\delta}$ in the region $U_{0,1} > 0$. As expected at small $|U_{0,1}|/J$ tunneling dominates and the product state $(a_1^\dagger/\sqrt{2} + a_2^\dagger/2 + a_3^\dagger/\sqrt{2})^N |\text{vac}\rangle$ is retrieved ($|\text{vac}\rangle$ is the vacuum state). This state transforms into phase (A), which for growing U_0 becomes the Fock state $|N/3, N/3\rangle$. Phase (C) remains the Fock state $|0, 0\rangle$ ($n_2 = N$), and the border (B)–(C) is characterized by a first-order “phase transition” [26], at which n_2 abruptly jumps from 0 to N . Figure 2(c) represents schematically phases (A)–(D).

Phase (B) is characterized by vanishing $\langle \hat{n}_2 \rangle$ and Δn_2 , and $\langle \hat{n}_1 \rangle = \langle \hat{n}_3 \rangle$. It strikingly reveals the nonlocal character of the DDI, similarly to the biconcave BECs predicted in [27], but with a much higher “contrast.” Note, however, that the actual ground state may significantly depart from $|N/2, N/2\rangle$, since $|\Delta \hat{\delta}|$ is significant at the (B)–(C) transition [Fig. 2(b)]. At $U_1 = 8U_0$, the ground state is a coherent state $(a_1^\dagger + a_3^\dagger)^N |\text{vac}\rangle$; i.e., coherence between the two extremal sites is preserved in spite of the absence of particles in site 2. This coherence is understood from (2), since for $U_1 = 8U_0$ there is no effective interaction between sites 1 and 3. Since $\langle \hat{n}_2 \rangle \ll 1$ due to the effective repulsive nearest-neighbor interactions ($U_1 - U_0 > 0$), sites 1 and 3 form an effective noninteracting two-well system coherently coupled by a second-order process through site 2 [with effective hopping $J_{\text{eff}} = J^2/7(N-1)U_0$]. Hence the coherent region extends inside (B) for $|U_1 - 8U_0| \leq J_{\text{eff}}$. Thus for larger NU_0 the coherent re-

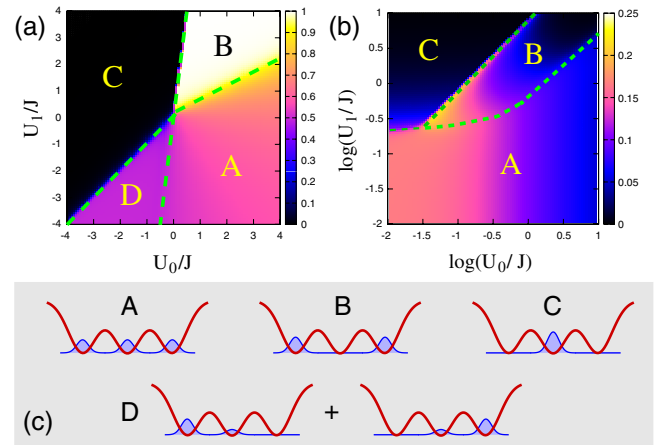


FIG. 2 (color online). (a) $\langle \hat{n} \rangle/N$ as a function of $U_{0,1}$ for $N = 18$. (b) $\Delta \hat{\delta}/N$ in logarithmic scale for $U_{0,1}$. The dashed lines show the boundaries between the classical phases (A)–(D) that are shown schematically in (c).

gion shrinks [reducing to the very vicinity of $U_1 = 8U_0$ as seen in Fig. 2(b)].

Such a 1–3 coherence has important consequences for the quantum dynamics, best illustrated by considering initially all particles at site 3. Interestingly, $\langle \hat{n}_{1,3} \rangle$ show perfect Josephson-like oscillations (with frequency $2J_{\text{eff}}/\hbar$), although for any time $\langle \hat{n}_2 \rangle = \Delta \hat{n}_2 \ll 1$. However, J_{eff} decreases with NU_0 , and hence the observation of this effect demands a mesoscopic sample, since otherwise the dynamics may become prohibitively slow. Off the $U_1 = 8U_0$ boundary, inside phase (B), the residual 1–3 interaction leads to a damping of the Josephson oscillations (connected to number squeezing). Eventually for $|U_1 - 8U_0| \gg J_{\text{eff}}$ self-trapping in 3 occurs.

Phase (D) is characterized by a large $\Delta \hat{\delta}$ and $\langle \hat{n}_2 \rangle \neq 0$, and two degenerated states: $n_3 = 0$ (i) and $n_1 = 0$ (ii). Strictly speaking, the exact ground state is provided by a MQS of these two states, but the gap between the ground state and the first excited one is vanishingly small ($\ll J$) even at the $U_1 = U_0 < 0$ boundary and for N as small as 18. Experimentally, the signature of phase (D) would thus consist in measuring large shot-to-shot fluctuations in $\hat{\delta}$, while never observing simultaneously atoms in both sites 1 and 3. At $U_1 = U_0 < 0$, states (i) and (ii) become coherent superpositions of the form $(a_1^\dagger + a_2^\dagger)^N |\text{vac}\rangle$ and $(a_2^\dagger + a_3^\dagger)^N |\text{vac}\rangle$, respectively. These superpositions may be understood from Eq. (2), which for $U_1 = U_0 < 0$ becomes

$$\hat{H} = -J[\hat{a}_2^\dagger(\hat{a}_1 + \hat{a}_3) + \text{H.c.}] + \frac{7|U_0|}{8}\hat{n}_1\hat{n}_3, \quad (3)$$

which describes a noninteracting two-well system if $n_1 = 0$ or $n_3 = 0$, leading to the coherent states (i) and (ii).

Hamiltonian (3) leads to an intriguing quantum dynamics characterized by the creation of MQSs. From an initial Fock state $|0, 0\rangle$ ($n_2 = N$), if a particle tunnels into site 1 (state $|1, 0\rangle$), a subsequent tunneling from 2 to 3 (state $|1, 1\rangle$) is produced with a bosonic-enhanced hopping rate $J\sqrt{N-1}$. However, the state $|1, 1\rangle$ has an interaction energy $7|U_0|/8$. Hence, if $J \ll 7|U_0|/8\sqrt{N-1}$, then the tunneling from 2 to 3 remains precluded. On the contrary, the hopping into 1 presents no energy penalty. As a result, if the first particle tunnels into 1, then a coherent 1–2 superposition is established. Of course, if the first particle tunnels into 3, then a 2–3 superposition occurs. Since the initial process is coherently produced in both directions, a MQS $|\Phi(t)\rangle|0\rangle + |0\rangle|\Phi(t)\rangle$ is formed, where $|\Phi(t)\rangle = \sum_{n=0}^N C_n(t)|n\rangle$, with the normalization condition $2\sum_{n=1}^N |C_n(t)|^2 + 4|C_0(t)|^2 = 1$ [25]. Figure 3(a) shows that $\langle \hat{n}_{1,3} \rangle(t)$ perform a coherent oscillation, which, however, damps for longer times. This damping is again a remarkable consequence of the nonlocal character of the DDI. Virtual hoppings of a single particle from site 2 into site 3 (1) induce a second-order correction of the energy of the states $|n, 0\rangle$ ($|0, n\rangle$): $\Delta E_n = 8J^2(N-n)/7|U_0|n$, which distorts the Josephson Hamiltonian, and leads to a signifi-

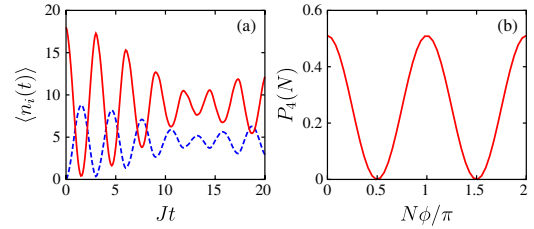


FIG. 3 (color online). (a) $\langle \hat{n}_{1,3}(t) \rangle$ (dashed line) and $\langle \hat{n}_2(t) \rangle$ (solid line), for $U_0 = U_1 = -100J$ and $N = 18$. (b) Probability $P_4(N)$ as a function of ϕ for the interferometric four-site arrangement (see text) with $N = 14$, $U_0 = U_1 = -100$, and $Jt = 2.7$.

cant damping after a time scale of the order of $\tau \sim 7|U_0|/8J^2N$ (in agreement with our numerics) [25]. At longer times, chaotic dynamics may even occur [28].

The three-well system hence acts as a MQS splitter under the mentioned conditions. We stress, however, that a MQS (although asymmetric) is still created [25], even for unequal hoppings J_{ij} for nearest neighbors, as long as $J_{12,23} \ll 7|U_0|/8\sqrt{N-1}$. We note also that if $U_1 \neq U_0$, a MQS is created if $|U_1 - U_0| \lesssim J$, but nearest-neighbor interactions enhance the damping in each MQS branch. If $|U_1 - U_0| \gg J$, bosons at site 2 remain self-trapped.

The MQS splitter opens fascinating possibilities beyond the three-well system, most relevantly in the context of Heisenberg-limited atom interferometry. We illustrate this possibility by considering a simple interferometer based on a four-well system [Fig. 1(b)]. Initially the bosons are at site 2 (which acts as the input port). Sites 1 and 3 play the role of the interferometer arms, whereas site 4 acts as the output port, where the interferometric signal is read out. We consider hoppings $J_{21} = J_{23} = J$, but $J_{34} = Je^{i\phi} = J_{43}^*$. We are interested in the ϕ sensitivity of the population at site 4. This arrangement is chosen for its theoretical simplicity (more general arrangements work along similar lines), although it may be implemented also in practice by means of Raman tunneling [29]. Under the MQS conditions [in this case $U_1 = U_0 < 0$ and $J\sqrt{N-1} \ll (2\sqrt{2}-1)|U_0|/2\sqrt{2}$], the system evolves into an entangled MQS formed by Fock states such that $n_i n_j = 0$ for next-nearest neighbors. It is straightforward to show that the probability to find N particles at site 4 depends explicitly on the phase ϕ as $P_4(N) \sim \cos^2(N\phi)$ [$P_4(n \neq N)$ are only indirectly ϕ dependent due to normalization]. Hence, $P_4(N)$ has a modulation of period $\delta\phi = \pi/N$ [Fig. 3(b)], contrary to the period $\delta\phi = \pi$ expected for independent single particles, allowing for a Heisenberg-limited interferometric measurement of the phase ϕ . This superresolution is an unambiguous signature of the coherent character of the MQS thus created [30,31]. $\langle \hat{n}_4 \rangle$ presents a similar modulation (but with poorer contrast). Calculations with a six-site arrangement provide similar results [25].

In the final part of this Letter we discuss experimental feasibility. Triple-well potentials as in Fig. 1 may be con-

trollably implemented with optical potentials. By superimposing, onto a single-beam optical trap which provides the xz confinement, a tightly focused beam (with a waist $\sim 1 \mu\text{m}$, see, e.g., [32]), one may create a tight “dimple” acting as one well. To realize a triple well (or even more complex configurations), several possibilities exist. Using an acousto-optic modulator (AOM) with several rf frequencies [33,34], several diffracted beams are created, whose intensity and position can be controlled independently. Another option using an AOM consists in toggling the dimple between several positions at high rate, to create almost arbitrary time-averaged potentials [35]. Such an implementation has several advantages: arbitrary, time-dependent energy offsets can be applied to the different sites; the intersite separation ℓ can be changed in real time, easing the preparation of a given atom number in each well (e.g., by performing evaporative cooling with different energy offsets in each site), and the detection of the population in each well (before imaging, V_0 may be increased to freeze out the dynamics and then ℓ increased, thus relaxing constraints on the imaging resolution).

We now evaluate J , U_0 , and U_1 for realistic experimental values. Although in our calculations we have just considered N up to 36, similar ground states are expected for larger N [but, as mentioned above, the observation of the quantum features at the (B)–(C) and (D)–(C) boundaries demands small samples]. In particular, consider a triple-well potential formed by three Gaussian beams of waist $1 \mu\text{m}$ separated by $\ell = 1.7 \mu\text{m}$. For a barrier height $V_0/h \simeq 2500 \text{ Hz}$, we obtain $J/h \sim 10 \text{ Hz}$, and the typical value of NU_1/J is then ~ 10 for $N = 2000$ ^{52}Cr atoms. The value of U_0 can be tuned, for a fixed geometry, by means of Feshbach resonances [4], so that one can explore, e.g., the first-order (B)–(C) “transition” with ^{52}Cr by varying U_1/U_0 . However, the MQS creation demands small samples, being hence more realistic with polar molecules. For example, for KRb molecules placed at a distance $\ell = 1 \mu\text{m}$ and maximally polarized ($d = 0.5 \text{ D}$) parallel to the joining line between the sites, $U_1/h \simeq -70 \text{ Hz}$. Under these conditions the MQS condition implies, for $N = 36$ molecules, J/h of a few hertz. Single-atom sensitivity has been achieved with fluorescence imaging [36], so that the relatively small values of N considered here should be detectable.

In summary, we have studied a simple system of dipolar bosons in a triple well, showing that the nonlocality of the DDI leads to qualitatively novel physics that may be explored with a high degree of control over all parameters via the trap geometry, dipole orientation, and Feshbach resonances. We have shown that the ground-state phases present abrupt crossovers induced by the nonlocal nature of the DDI, which may be explored with ^{52}Cr BECs. In addition, the dynamics presents intriguing new scenarios, especially for the case of polar molecules, including the dynamical creation of MQSs, which may be employed for Heisenberg-limited interferometry.

We thank M.K. Oberthaler, H.P. Büchler, D. Guéry-Odelin, and E. Demler for useful discussions. We acknowledge support by the DFG (QUEST and SFB/TRR 21), the ESF (EUROQUASAR), and the EU (Marie-Curie Grant No. MEIF-CT-2006-038959 to T.L.).

-
- [1] I. Bloch, J. Dalibard, and W. Zwerger, *Rev. Mod. Phys.* **80**, 885 (2008).
 - [2] M. A. Baranov, *Phys. Rep.* **464**, 71 (2008).
 - [3] T. Lahaye *et al.*, *Rep. Prog. Phys.* **72**, 126401 (2009).
 - [4] T. Lahaye *et al.*, *Nature (London)* **448**, 672 (2007).
 - [5] T. Koch *et al.*, *Nature Phys.* **4**, 218 (2008).
 - [6] T. Lahaye *et al.*, *Phys. Rev. Lett.* **101**, 080401 (2008).
 - [7] J. Metz *et al.*, *New J. Phys.* **11**, 055032 (2009).
 - [8] M. Vengalattore *et al.*, *Phys. Rev. Lett.* **100**, 170403 (2008).
 - [9] M. Fattori *et al.*, *Phys. Rev. Lett.* **101**, 190405 (2008).
 - [10] S. E. Pollack *et al.*, *Phys. Rev. Lett.* **102**, 090402 (2009).
 - [11] K.-K. Ni *et al.*, *Science* **322**, 231 (2008).
 - [12] J. Deiglmayr *et al.*, *Phys. Rev. Lett.* **101**, 133004 (2008).
 - [13] K. Góral, L. Santos, and M. Lewenstein, *Phys. Rev. Lett.* **88**, 170406 (2002).
 - [14] C. Menotti, C. Trefzger, and M. Lewenstein, *Phys. Rev. Lett.* **98**, 235301 (2007).
 - [15] M. Albiez *et al.*, *Phys. Rev. Lett.* **95**, 010402 (2005).
 - [16] B. Xiong *et al.*, *Phys. Rev. A* **79**, 013626 (2009).
 - [17] M. Asad-uz-Zaman and D. Blume, *Phys. Rev. A* **80**, 053622 (2009).
 - [18] A. Argüelles and L. Santos, *Phys. Rev. A* **75**, 053613 (2007).
 - [19] D. W. Wang, *Phys. Rev. Lett.* **98**, 060403 (2007).
 - [20] C. Trefzger, C. Menotti, and M. Lewenstein, *Phys. Rev. Lett.* **103**, 035304 (2009).
 - [21] See, e.g., S. Haroche and J.-M. Raimond, *Exploring the Quantum* (Oxford University Press, Oxford, 2006), and references therein.
 - [22] J. I. Cirac *et al.*, *Phys. Rev. A* **57**, 1208 (1998).
 - [23] T.-L. Ho and C. V. Ciobanu, *J. Low Temp. Phys.* **135**, 257 (2004).
 - [24] M. W. Jack and M. Yamashita, *Phys. Rev. A* **71**, 023610 (2005); P. Buonsante, V. Penna, and A. Vezzani, *Phys. Rev. A* **72**, 043620 (2005); J. Javanainen and U. Shrestha, *Phys. Rev. Lett.* **101**, 170405 (2008).
 - [25] See supplementary material at <http://link.aps.org/supplemental/10.1103/PhysRevLett.104.170404> for more details.
 - [26] Strictly speaking, one deals only with a crossover, since the system has a finite size.
 - [27] S. Ronen, D. C. E. Bortolotti, and J. L. Bohn, *Phys. Rev. Lett.* **98**, 030406 (2007).
 - [28] P. Buonsante, R. Franzosi, and V. Penna, *Phys. Rev. Lett.* **90**, 050404 (2003).
 - [29] D. Jaksch and P. Zoller, *New J. Phys.* **5**, 56 (2003).
 - [30] M. W. Mitchell *et al.*, *Nature (London)* **429**, 161 (2004).
 - [31] P. Walther *et al.*, *Nature (London)* **429**, 158 (2004).
 - [32] Y. R. P. Sortais *et al.*, *Phys. Rev. A* **75**, 013406 (2007).
 - [33] Y. Shin *et al.*, *Phys. Rev. Lett.* **92**, 050405 (2004).
 - [34] B. Fröhlich *et al.*, *Rev. Sci. Instrum.* **78**, 043101 (2007).
 - [35] K. Henderson *et al.*, *New J. Phys.* **11**, 043030 (2009).
 - [36] R. Bücke *et al.*, *New J. Phys.* **11**, 103039 (2009).